IN-BEAM TEST OF THE TIGRESS PROTOTYPE DETECTOR

IN-BEAM TEST OF THE TIGRESS PROTOTYPE DETECTOR

By
LESLEY MARIA WATTERS, B.Sc

A Thesis
Submitted to the School of Graduate Studies
in Partial Fulfillment of the Requirements
for the Degree
Master of Science

McMaster University

MASTER OF SCIENCE (2005) McMaster University
(Physics) Hamilton, Ontario

TITLE: In-Beam Test of the TIGRESS Prototype Detector

AUTHOR: Lesley M. Watters, B.Sc. (University of Liverpool)
SUPERVISOR: Professor J.C. Waddington
NUMBER OF PAGES: viii, 51

Abstract

This thesis describes the preparations for the first in-beam test of a new type of gamma-ray detector, which will be part of the TIGRESS array of segmented high-purity Germanium clover detectors.

Gamma rays emitted from a moving nucleus are Doppler-shifted leading to a broadening of the measured photo-peak. Through a determination of the interaction position in the crystal, it is anticipated that most of the resolution may be recovered with these detectors. In order to test this prediction, the detector has been tested in an experiment. Prior to this test, a "pre-test" was done with a conventional detector. The reasons for the choice of the reaction for the pre-test, the description of the experiment and its results and the lessons learned will be presented.

Acknowledgements

I am deeply grateful to my supervisor, Dr J.C. Waddington, for giving me the opportunity to study in Canada and also for his patience and guidance throughout my endeavours at McMaster University. I am also grateful to the faculty and staff members of the Physics & Astronomy department.

I would like to thank the staff at Triumf, and my colleagues in the Physics Department at the University of Guelph, who have assisted in my education of all things nuclear and made me feel welcome.

My thanks also go to my friends and colleagues in the Physics & Astronomy department at McMaster University, particularly Kristin Woodley, Pamela Klaassen, Kiri Nichol, and Steve Bickerton for their reassurances, encouragement and advice.

My deepest gratitude and love go to my mother, my husband Robin, and my daughter Charlotte for their love, support, patience and encouragement throughout my University life.

Contents

List of Figures

List of Tables

Chapter 1

Introduction

The test carried out in this work arose from a requirement identified by the review team involved with the TIGRESS project.

1.1 TIGRESS

TIGRESS is the acronym for the TRIUMF-ISAC Gamma-Ray Escape Suppressed Spectrometer. It will consist of 12 segmented high-purity Germanium crystal clover detectors, arranged in a nearly spherical pattern. Each clover will be equipped with anti-Compton suppression shields, which improve the peak-to-background ratio by suppressing Compton-scattered events. The array will be adjustable to several geometrical arrangements, depending on the needs of individual experiments. It will also be possible to couple it with auxiliary detectors, specific to experimental requirements.

The most efficient way to detect gamma rays is to have large-volume detectors positioned as close as possible to the gamma ray source. However, as in-beam experiments usually result in γ-rays being emitted by nuclei recoiling with typical

velocities of $v \sim 5\%$ of the speed of light, c, at Coulomb barrier facilities and up to $v \sim 70\%$ of c, at fragmentation facilities, the Doppler broadening of the gamma ray energy causes degradation of resolution (see Section 2.1). To overcome this challenge, segmenting the outer electrical contacts of the HPGe detector makes it possible to pinpoint the position of the event within the crystal. The result of this is to improve the resolution of the gamma ray measurement [Sve 04].

When they conducted their review in September 2004, the NSERC TIGRESS Project Technical Review Team requested that the "collaboration should carry out end-to-end tests of the HPGe detector during an in-beam experiment" [Tig 04]. To this end, it was decided that a 'pre-test' be carried out using a conventional Ge detector. This pre-test would be used to commission a new beam-line, and determine whether or not a proposed beam-target combination were suitable. Since Doppler correction was not possible with this detector, it was placed directly in front of beam/target so as to minimize the Doppler problem. During the subsequent full test, data were collected from all contacts so that energy and position information could be determined for each event. Once the collected data have been fully analysed, it will become clear whether or not computer simulation programs correctly predict the outcome of a real experiment and the tests will also illustrate whether or not the new detectors can be used to correct for serious Doppler broadening.

1.2 The TRIUMF-ISAC Facility

TRIUMF is the Tri University Meson Facility located on the University of British Columbia campus in Vancouver. The acronym is somewhat outdated as there are now more than three universities in the collaboration and the laboratory is certainly not entirely a meson facility. ISAC is the Isotope Separator and Accelerator, which utilizes the proton cyclotron beam at TRIUMF to produce radioisotopes. A beam of 500MeV protons bombards a suitable target; the resulting radioisotopes are then separated, providing a low-speed beam of radioactive particles. The job of ISAC is to speed up these beams to much higher velocities in a linear accelerator (linac), providing radioactive beams of mass range up to A=30 and energy up to 1.5 MeV/A (largely for use in nuclear astrophysics experiments). An upgrade of ISAC to ISAC II is currently in progress with the installation of a Charge State Booster (CSB), which will increase the accelerated mass range up to 150 and the energy up to 6.5 MeV/A [Tri 02]. The higher energy will make the facility, shown in Figure 1.1, suitable for a wide range of applications to nuclear structure physics, nuclear reactions, and nuclear astrophysics.

Figure 1.1 ISAC II Building at TRIUMF, Vancouver [Tri 03a]

Chapter 2

Background

There are a number of factors that influence the decision on which reaction to use, to fulfill the requirements of this experiment. The gamma-ray transition should be at relatively high energy, with a large Doppler shift and the decay should be much faster than the slowing-down time in a target. Ideally, the gamma energies should be close to the real gamma energies that TIGRESS will be detecting. The transition must be capable of being produced with a stable beam of less than 1.5MeV/A and with A<30 (restrictions of the ISAC facility). The direction of motion of the emitting nucleus must be known; a particle capture reaction is particularly good because the recoil direction is known. Manufacture of the required target should also be feasible and, hopefully, not too difficult to achieve.

Beam time is in great demand by many different scientists at all major nuclear research facilities. It is therefore prudent to design an experiment whereby the minimum amount of beam time is required. To this end, an in-beam test should maximize the amount of gamma rays being emitted, in order to reduce the length of time needed to acquire data.

2.1 Doppler Broadening

One reason for segmenting clover detectors is to reduce the effect of the Doppler broadening. The gamma rays emitted by a nucleus recoiling at ~2-5% the speed of light have an appreciable Doppler shift, which causes Doppler broadening of the spectral peaks. The energy of the photon, E_γ, depends on its angle with respect to the recoil direction, θ. To find the energy:

$$E_\gamma \cong E_o(1+\tfrac{v}{c}\cos\theta) \tag{2.1}$$

where E_o is the energy of a photon emitted from a stationary nucleus. Since θ varies across the face of the detector, photons of a range of energies enter the detector. Segmentation leads to a reduction in the opening angles of the crystal. The isolated hit probability, which accounts for the possibility of a second gamma ray hitting the same detector, is also increased using segments. It may be possible to distinguish between two gamma rays hitting the same detector, and a gamma ray scattering between adjacent crystals.

2.2 Resonance

A resonant capture reaction with no emitted particles results in a recoiling nucleus of known direction (the beam direction). Some reactions have a large enough resonance

strength to be used. Low binding energies are required for good resonances, so that the level density is small.

The reaction chosen for this experiment was $p(^{23}Na, \gamma)^{24}Mg$ as it has a low binding energy, and a ^{23}Na beam is easy to produce at Triumf. Resonance happens when the energy of the initial system matches the energy of an excited state of the final system whose structure is favourable towards formation by, in this case, the original system plus a proton. Therefore, the need for a suitable initial beam, and a target containing hydrogen (to gain the proton) is required. The ^{23}Na beam was tested with different targets, primarily to determine whether or not they contained hydrogen. The $2^+ \rightarrow 0^+$ transition in ^{24}Mg has an energy of 1368keV and a half-life of 1.35ps. If the recoils travel at 5% of c then they will travel ~0.2μm before they decay. Therefore, the target thickness should be greater than 0.2μm in order to stop the recoils. The test will also highlight if this is the best combination of beam/target to thoroughly test the prototype detector and fulfill the requirements of the review team.

The $p(^{23}Na, \gamma)\ ^{24}Mg$ reaction has been studied in detail and the quoted paper contains a table of energies and strengths of 23Na+p resonances [Mey 72].

The thickness of the target also impacts on the yield of resonances detected. With a thin target the beam energy loss is small and, therefore, populates only a few

resonances. The recoils move out of the target and typically decay in vacuum with little variation in recoil velocity. A thick target has a large energy loss and many resonances are populated. There is a variation in velocities as the majority of the reactions take place in the target or any recoils decay before they leave the target.

2.2.1 Theoretical calculations

By adapting the method used by a colleague involved in the TIGRESS collaboration [Les 04], the theoretical yield of gammas, Y_{calc}, was calculated using the following formula:

$$Y_{calc} = \frac{1}{\Sigma}\frac{\lambda^2}{2}\omega\gamma \tag{2.2}$$

where Σ is the stopping power per atom of ^{24}Mg on Ti, the value taken from published Nuclear Data Tables [Nuc 70], λ is the centre of mass wavelength of the projectile and $\omega\gamma$ is the strength of the resonant capture, given by the following formula:

$$\omega\gamma = \frac{(2J+1)}{(2I_o+1)(2i_o+1)}\frac{\Gamma_\gamma\Gamma_p}{\Gamma} \tag{2.3}$$

where J is the spin of the resonance of the system, I_o is the spin of the projectile (3/2 for ^{23}Na) and i_o is the spin of the target (1/2 for hydrogen). By rearranging the formula, the rest of the resonance unknowns can be extracted and are given in Table 24.7 of [NIM 71] thus:

$$8\omega\gamma = (2J+1)\frac{\Gamma_\gamma \Gamma_p}{\Gamma} \tag{2.4}$$

which has a value of 42 for the 1.42 MeV resonance. Γ_γ is the partial width for the gamma, Γ_p for the proton and Γ is the total partial width. The centre of mass wavelength, λ, can be calculated from the de Broglie (laboratory) wavelength. Figure 2.1 demonstrates the difference between the lab frame and the centre of mass frame. The laboratory frame is from the point of view of the observer. The red particle comes in and collides with the blue particle; both move off with a shared velocity. The centre of mass frame deals with one point in the system that moves as if all the mass of the system acts at that one point. As this is a perfectly inelastic collision, there is no relative velocity in the centre of mass frame and the two particles are "stuck together" at the centre of mass.

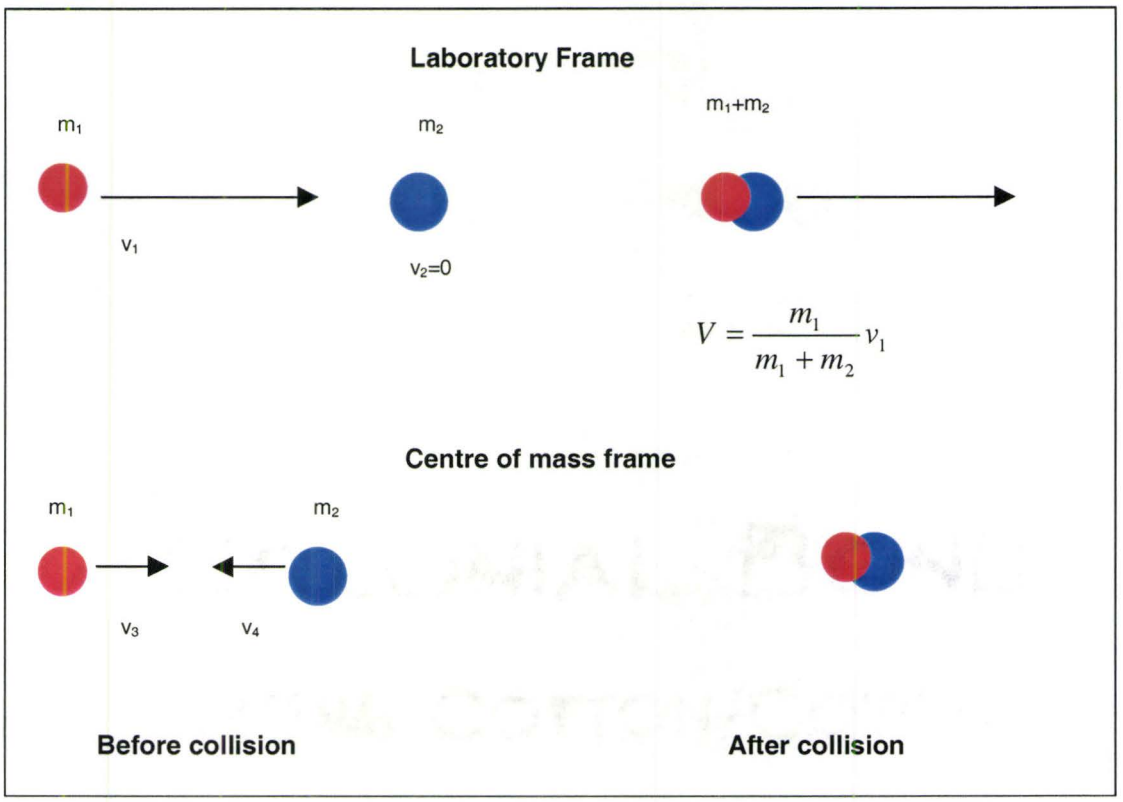

Figure 2.1 Schematic of lab frame v centre of mass frame

By manipulation,

$$V = \frac{\sqrt{2Em_1}}{m_1 + m_2^{\,2}} = v_{cm} \tag{2.5}$$

where the definition for V is given in Figure 2.1 and E is the beam energy (m_1 in the lab frame).

The velocity of m_1 in the centre of mass frame:

$$v_{1cm} = v_1 - v_{cm} = \sqrt{\frac{2E}{m_1}} \frac{m_2}{m_1 + m_2} \tag{2.6}$$

The energy of m_1 in the centre of mass frame:

$$E_{1cm} = \frac{Em_2^2}{(m_1 + m_2)^2} \tag{2.7}$$

For the ^{23}Na beam (m_1) on a proton (m_2):

$m_1 = 22.98977u = 3.85x\ 10^{-26}kg$

$m_2 = 1.67262158 \times 10^{-27}kg$

$E = 1.416MeV\ x\ 23 = 5.2x10^{-12}J$

$$\lambda = \frac{h(m_1 + m_2)}{m_2} \frac{1}{\sqrt{2m_1 E}} \tag{2.8}$$

giving a centre of mass wavelength, $\lambda = 6.3x10^{-24}$m.

The resonance energy is 1.42 MeV so a beam energy of 1.43 MeV/u is sufficiently high to induce the resonance. The bombarding energy is the energy/u

multiplied by its isotopic number (23), giving an energy of 32.89 MeV. It is well known that the resonance line at 1.42 MeV decays to the 4^+ state 95% of the time, and then decays to the 2^+ state completely [Bro 79].

2.3 Fusion evaporation reactions

Another way to maximize the gamma ray yield is to utilize fusion evaporation reactions and choose a reaction with a large cross-section. Fusion evaporation reactions occur when the target and projectile nuclei fuse together to form a compound nucleus. The level density is often very high and many overlapping levels are populated, making it more difficult to identify specific reaction energies.

The projectile must have a large enough energy to overcome the Coulomb barrier, so that the fusion evaporation reaction may take place. The newly formed compound nucleus is unstable and will decay. There are various ways that the nucleus can lose its excitation energy including fission and emission of particles (p, n, α). If the angular momentum transfer is too large, a compound nucleus will be unable to form because rapid rotation would overcome the short-range attraction of the nuclear force [Gre 99].

2.4 Coulomb Excitation

Coulomb excitation, or coulex, occurs when a nucleus is bombarded by heavy ions of sufficient energy to excite it but not to penetrate the Coulomb barrier and cause nuclear reactions to take place. By raising the energy of the nucleus in this way, the gamma rays that are emitted during de-excitation can be observed and the nucleus identified.

2.5 Beam Production

The TRIUMF cyclotron is a particle accelerator, which can transport up to 100 μA of a 500MeV proton beam to various target stations in the TRIUMF facility, one being the ISAC Experimental Hall. Spallation provides a large variety of short-lived isotopes, which can then be transported to experimental areas in the ISAC Experimental Hall. Figure 2.2 shows the layout of the TRIUMF facility and the directions of the beam lines to the various experimental halls and areas.

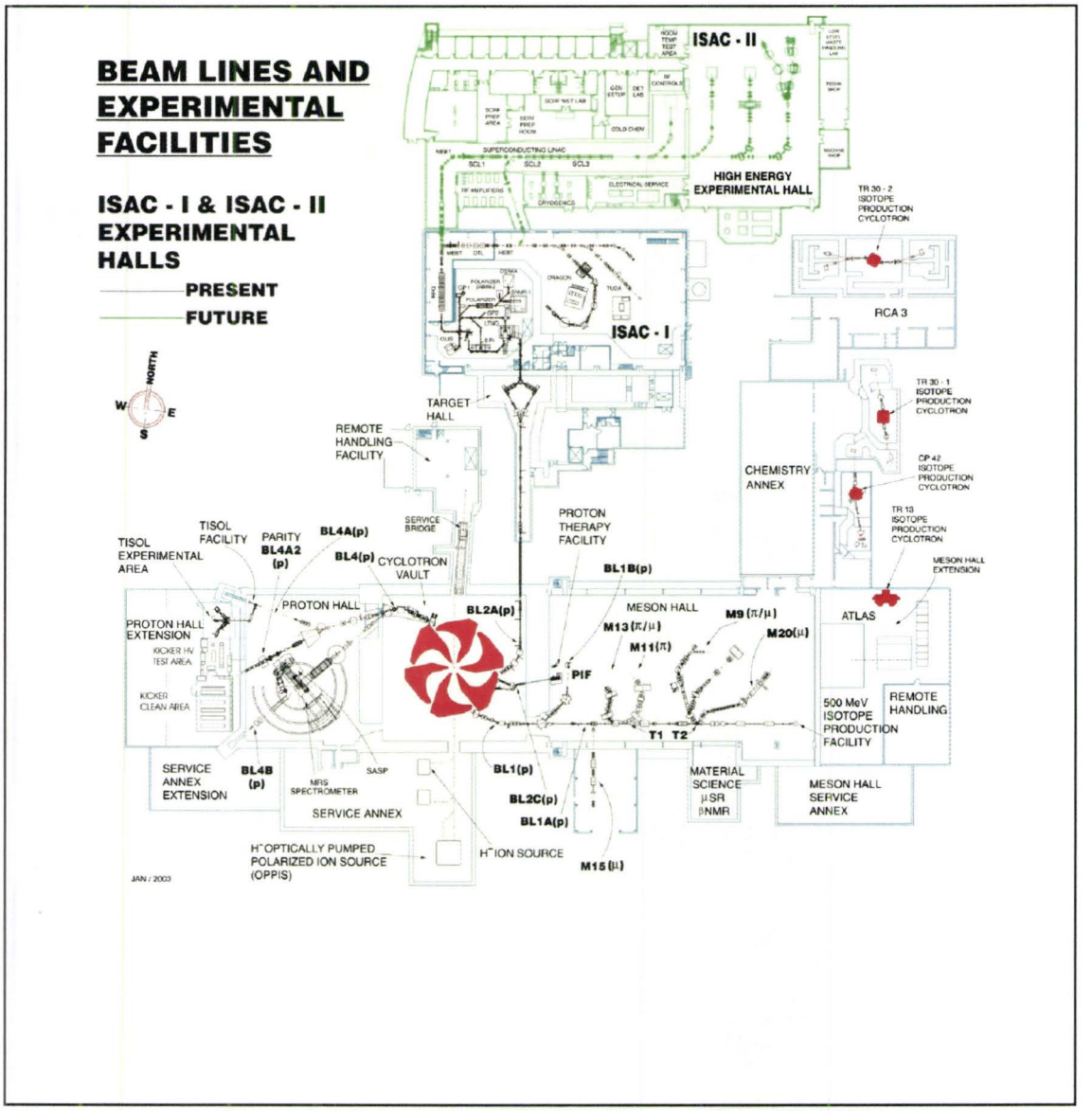

Figure 2.2 Schematic of TRIUMF beam lines [Tri 02b]

Foil targets, including tantalum and niobium, are regularly used in operation at proton currents as high as 40 μA. The targets are maintained at high temperature by the

proton beam and an external heated tube. The products diffuse from the target and are transferred to an ion source.

A magnetic mass separator, with a resolution up to $1/10^4$, selects a particular isotope from the ion source. These selected isotopes are available at energies up to 60keV. They can be delivered to either a system of linear accelerators or to a variety of experimental stations through a beam line. The beam is focused and steered using quadrupoles and dipoles. Low-energy experimental facilities include the 8π detector, which is regularly used by the Canadian members of the TIGRESS collaboration.

The linacs consist of a rf quadrupole (RFQ), which focuses the beam, and a five-tank drift tube linac (DTL), which accelerates the beam to higher energies. There is a minimum injection energy of 2keV/A for acceleration of a singly charged isotope from either the target ion source (stable and radioactive ion beams (RIBs)), or from an offline ion source (OLIS, stable beams). The accelerated beam energy is continuously variable from 0.15 to 1.5 MeV/A. A series of bunchers and choppers permit the time between rf beam buckets and/or the time focus at the experiment to be adjusted. Bunchers consist of a rf electrical field orientated in the direction of the beam. By adjusting the voltage, the front end of the beam can be slowed down to allow the back end to "catch up". This reduces the time spread of the beam pulse and keeps it within the allowed time frame for that pulse. Choppers consist of two electrical plates either side of the beam so that a

voltage can be set up across the beam; by changing the potential difference between the plates, the beam can be deflected sideways so that it does not reach the experimental apparatus. When used in conjunction with a buncher, this has the effect of regulating the pulses of the beam. The accelerated beam quality is such that the beams have an energy spread of less than 0.1% and selectable intervals of 28, 85 or 170 ns between beam bursts [Tri 02].

There are two main types of beam produced at TRIUMF's ISAC facility. The first uses the ISOL technique to produce radioactive beams. The second uses the offline ion source (OLIS) for the production of stable beams. For the test experiment, the second type of beam was used, as it was not necessary to use a radioactive beam for this particular experiment. Both types of beam production will be described here.

2.6 Isotope Separation Online (ISOL)

There are four elements that make up the ISOL system. They consist of a primary production beam, a target/ion source, a mass separator, and a separated beam transport system. Together these elements act as the source of radioactive ion beams to be provided to the accelerator or the low-energy experimental areas.

The primary production beam for the ISOL system is the 500MeV proton beam from the H^- cyclotron at TRIUMF. Beam intensity up to 100μA can be accommodated. Radionuclides are produced in the target/ion source assembly, transferred to the ion source, ionized and then extracted to form an ion beam. With high energy protons the three principal reactions used are: spallation, fission and target fragmentation, which cover almost the entire chart of the nuclides.

The ISOL method involves bringing the reaction products to rest before releasing them from the target material. This needs to be done as quickly as possible to minimize decay of the products and to prevent delay due to slow diffusion release or slow effusion from collisions. A low vapour pressure target material is heated to a sufficiently high temperature at which the nuclei of interest are released by diffusion and effusion process toward the ion source. The atoms are then ionized and extracted to form an ion beam and a mass separator is used to obtain separation.

A mass separator is used to separate out unwanted ions from the beam, which are usually higher in intensity by several orders of magnitude than the ones of experimental interest. The mass separator has a mass resolving power of $m/\delta m$ of the order of 10,000, which is adequate for many of the experiments carried out at TRIUMF. There are two stages of the mass separator, which results in most of the particles having the same

momentum but different mass being rejected, leaving the ions needed for the experiment [Bri 01].

2.6.1 Offline Ion Source

The Offline Ion Source (OLIS) was used to produce a stable beam in this experiment. Sodium metal was vaporized by heating the sodium reservoir of the surface ionization source. The Na atoms ionize on the inner wall and pass through a porous rhenium plug, as Na^+ ions as shown in Figure 2.3.

Atoms of elements with low ionization potential (I) are converted to singly charged ions when they come into contact with a metal surface of high work function (Φ). Sodium has a low ionization potential and Rhenium has a high work function (Φ = 5.1 eV) so, in theory, 100% ionization efficiency is possible.

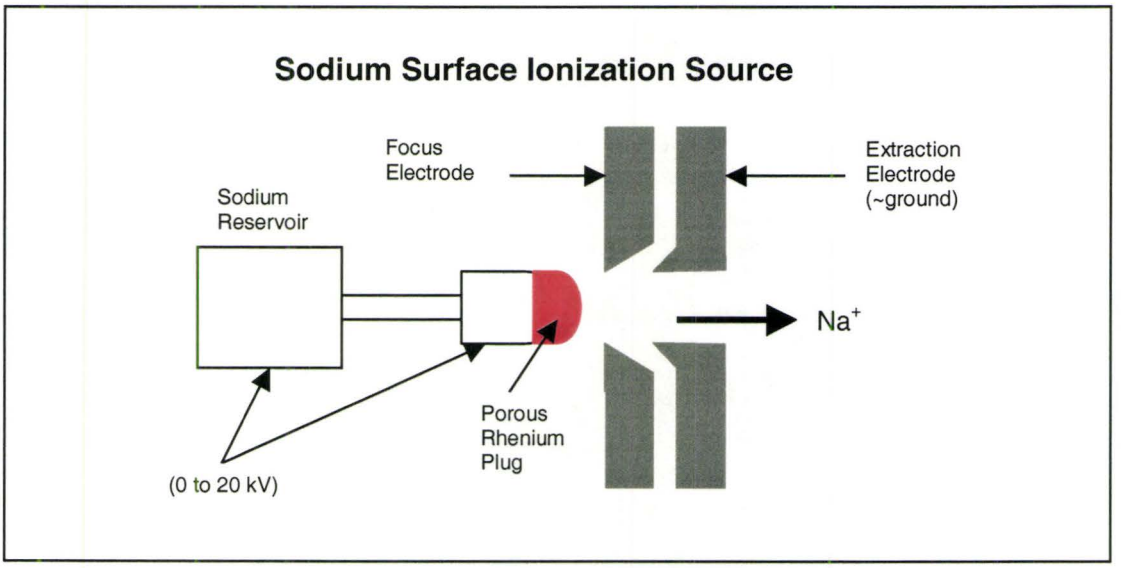

Figure 2.3 Schematic of OLIS used in test. Adapted from [CEA 95].

Originally, the off-line ion source was developed to evaluate potential ion sources for use in the online system. There was a need for a system that could be adjusted during operation, as the ion sources can only be handled remotely in hot cells during on-line operation. It is capable of operating over a range of beam energies, currents and masses. Optimum beam extraction is achieved by tuning the voltages of the component electrodes rather than by adjusting the relative positions of the ion source and extraction electrode, creating a more dynamic and responsive system. The OLIS system is now also used to conduct test experiments, such as the one described in this thesis, which can be done with a stable beam, rather than a more complex experiment requiring production of a radioactive ion. It is also used to tune the steering elements of the beam line, in

preparation for an experiment, and can be thought of as a preliminary test of the system to be used [Dom 98].

2.7 High purity Germanium detectors

High purity Germanium detectors (HpGe) employ the principles of semiconductors to achieve the high resolution required in gamma spectroscopy. They are, basically, large reverse-biased p-n junction diodes that have a region of net zero charge, known as the depletion region, caused by the migration of electrons from the n-type material and holes from the p-type material. The net positive charge on one side of the junction and the net negative charge on the other side set up an electric field gradient across the depletion region. Any gamma rays emitted in nuclear transitions interact via three different processes, depending on their energy. In each process, the energy is transferred to electrons in the Germanium, giving rise to electron-hole pairs. These processes are the photoelectric effect, Compton scattering and pair production.

The depletion region in the detector is the active region so the bigger the better. Unfortunately, natural Germanium can only maintain a depletion region of a few mm before electrical breakdown occurs. However, high purity Germanium crystals can be grown, which have an impurity of 1 part in 10^{12} and result in detectors with a much larger

depletion region. HPGe detectors are operated at temperatures of around 77 K, in order to reduce noise from electrons, which may be thermally excited across the small band gap in Germanium (0.67 eV) at room temperature. The low temperature is achieved through thermal contact of the Germanium crystal with a dewar of liquid nitrogen, using a copper rod, known as a cold finger.

The active volume of a HPGe detector can be further increased by rounding off the corners, resulting in a more uniform electric field inside the detector and an active volume in the region of 400 cm^3. Also, a typical detector used in gamma spectroscopy has the n contact on the inside and the p contact on the outside (known as an n-type detector). The reason for this is that the p contact is much thinner than the n type and is less likely to attenuate the incident radiation. A p-type detector, where the n contact is on the outside and the p contact on the inside would be more susceptible to neutron damage; the neutron interaction will cause more p-type material to form and will alter the band gap in the material, degrading the efficiency of the detector. It is therefore less suitable as a detector [Kee 99].

2.7.1 Clover Detectors

A clover detector consists of four coaxial n-type Germanium crystals, arranged like a four-leafed clover, hence the name. This arrangement results in a much larger

volume of Germanium. Each of the four segments may be divided into four longitudinally and, for the TIGRESS detectors, the crystals are further segmented transversely to produce 8 outer-contact segments for each crystal and a total of 32 segments per clover [Scr 04]. A representation of a clover detector is shown in Figure 2.4.

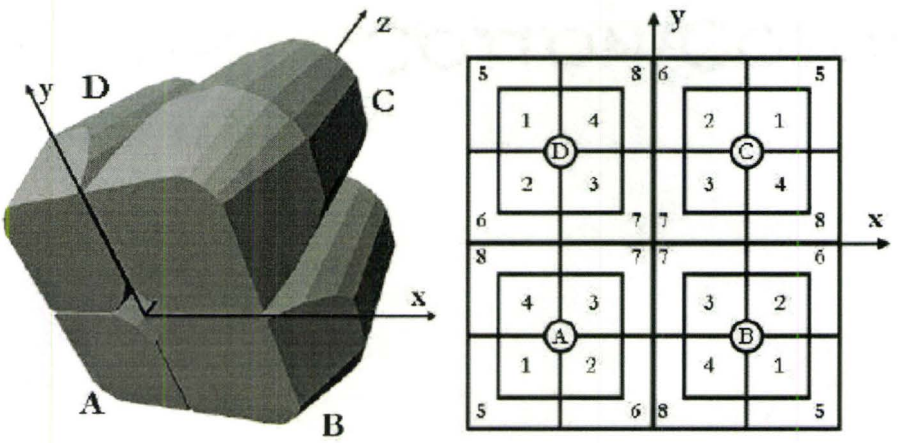

Figure 2.4 Representation of a TIGRESS clover detector. The crystals are labelled A (blue), B (green), C (red), and D (white), relative to the *x, y, z* coordinate system shown. The diagram on the right shows the segment labelling. Within each crystal the outer segments are labelled 1, 2, 3, 4 (front) and 5, 6, 7, 8 (back). Adapted from [Sve 04].

Without the segmentation, the larger clover detectors would suffer from severe Doppler broadening. The segmentation allows good energy resolution (smaller opening angles) while maintaining large detector efficiency.

The crystals are held by the rear side, thus reducing the amount of material around the detector and improving the peak-to-background response. This also enables close

packing of the crystals, which are mounted in a common cryostat of tapered rectangular shape.

Pulse shape analysis is also possible with this type of detector. Gamma rays scattering at different places in the crystal result in a variety of pulse shapes. This will allow even better position resolution than that resulting from single segments alone. Linear polarization of photons may also be made, where the detector can be used as a polarimeter.

Chapter 3

Preparation

3.1 Experimental Setup

Figure 3.1 shows the layout of the ISAC Experimental Hall. This experiment was set up at the end of the zero degree beam line after the HEBT across the top of the diagram.

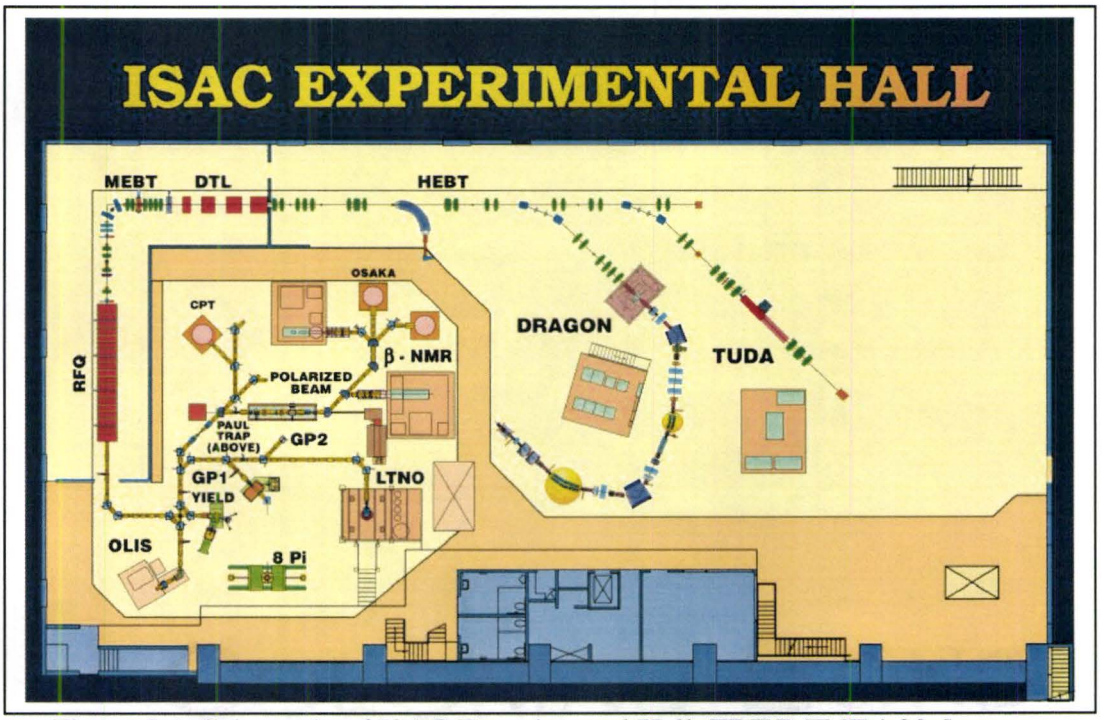

Figure 3.1 Schematic of ISAC Experimental Hall, TRIUMF [Tri 02a]

Figure 3.2 shows a schematic of the experimental setup.

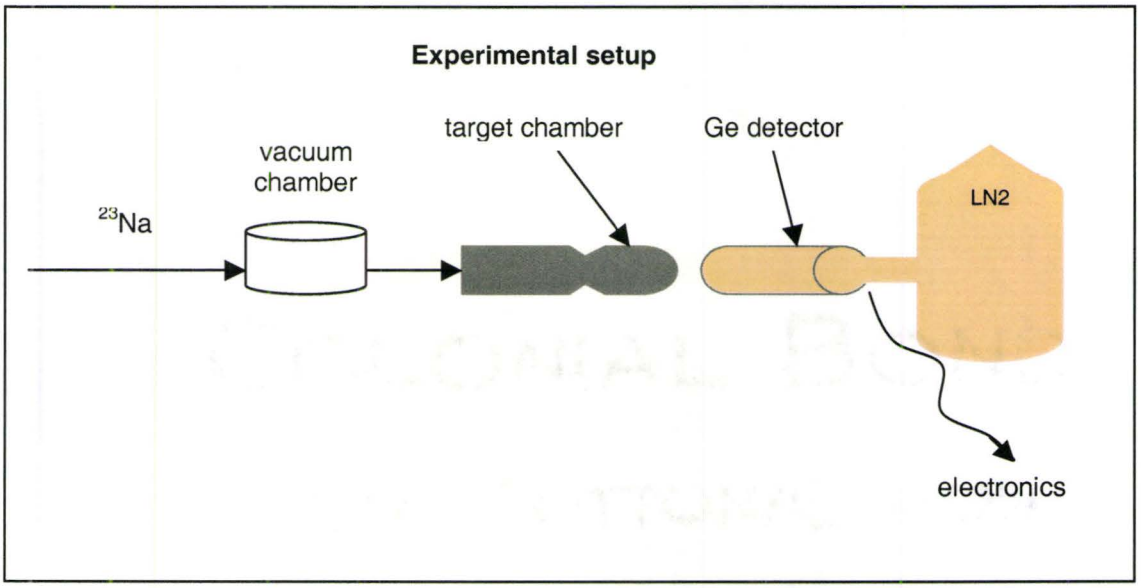

Figure 3.2 Schematic of experimental setup.

The Ge detector was placed as close to the target chamber as possible, while still being able to gain access to the chamber.

Figure 3.3 is a schematic of the orientation of the experiment. The target is placed in a holder, which can house up to four targets at once. The target shown is titanium hydride.

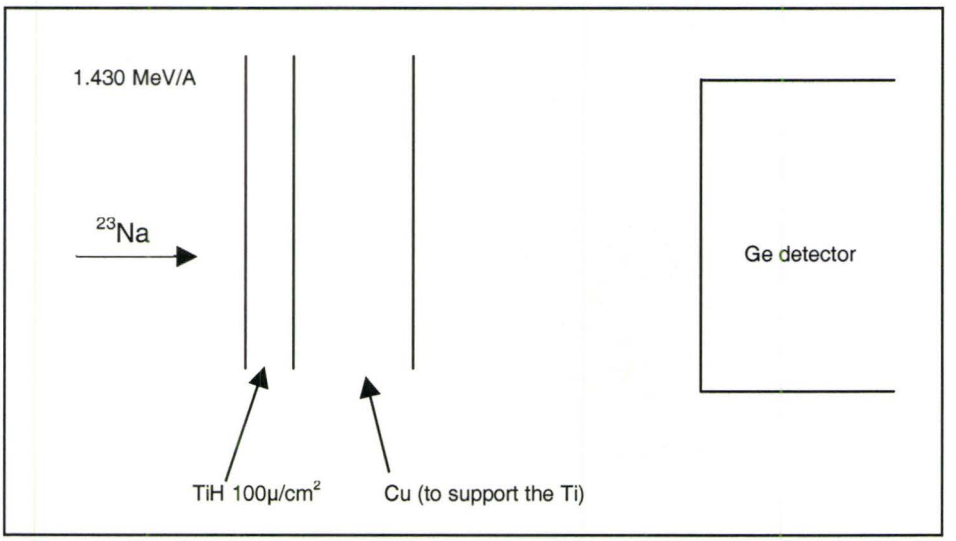

Figure 3.3 Schematic of experimental orientation

The holder for the targets is shown in figure 3.4, and figure 3.5 shows how the holder fits into the target chamber.

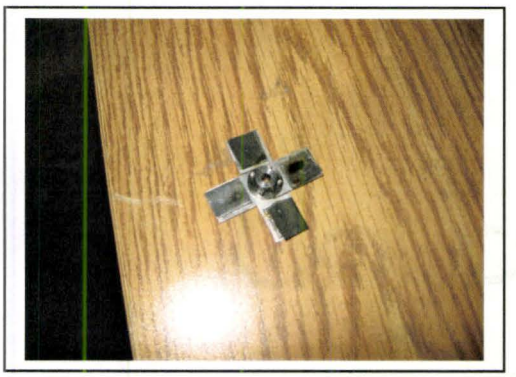

Figure 3.4 Image of target wheel

Figure 3.5 Target wheel and chamber

By mounting targets in a wheel, up to four targets can be placed separately in the beam by rotating a dial on the outside of the target chamber. Of course, if more than four targets are required, the beam must be turned off and the system vented before the target wheel can be removed from the chamber.

3.1.1 Beam Selection

As detailed in Chapter 2, the selection of a reaction to maximize gamma rays is paramount if the experiment is to be a success. As the $p(^{23}Na, \gamma)^{24}Mg$ reaction has the required resonance strengths, a beam of sodium was the obvious choice.

3.1.2 Target Specifications

A kinematic representation of the particles is useful here, if the Doppler shift is to be calculated.

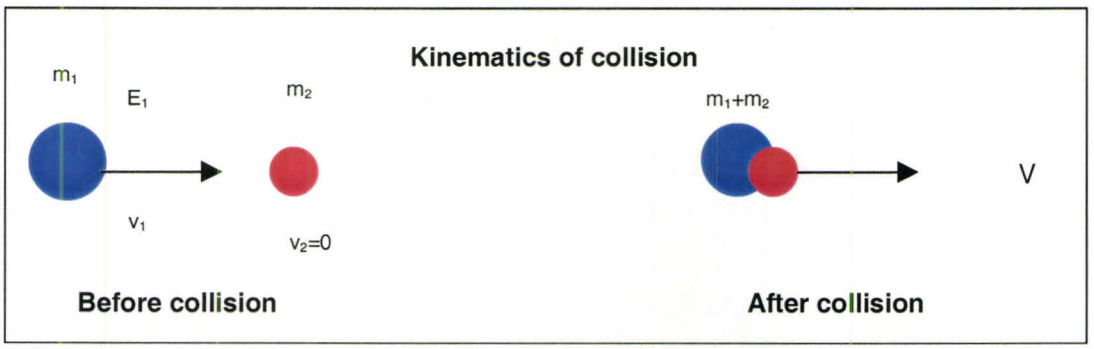

Figure 3.6 Diagram of collision kinematics

From conservation of momentum:

$$m_1 v_1 = (m_1 + m_2)V = p_1 \tag{3.1}$$

and by using:

$$T = \tfrac{1}{2} m_1 v_1^{\,2} = \tfrac{1}{2} \frac{(m_1+m_2)^2}{m_1} V^2 = E_1 \tag{3.2}$$

the following formula can be derived:

$$\frac{V}{c} = \frac{1}{(m_1 + m_2)} \sqrt{\frac{2E_1 m_1}{c^2}} \tag{3.3}$$

Equation 3.3 may be used to calculate the recoil velocity immediately after the collision. m_1 is the mass of the Na beam (22.98977 U), m_2 is the mass of the proton ($1.67262158 \times 10^{-27}$kg), making ^{24}Mg. With a beam energy of 1.43MeV/A (E_1), a recoil speed for the nucleus of 5% the speed of light was calculated. The half-life of the 2^+ ^{24}Mg state at 1.369MeV is 1.35ps so if the velocity is 5%c, the distance the recoils move in a vacuum before they decay is 0.2μm. It is unnecessary to work out the distance travelled in the copper (the actual thickness of the copper was 100μm), as long as it is at least as thick as 0.2μm to ensure the nuclei are stopped in the material. If shorter-lived nuclei decay in the material, their energy is boosted by:

$$E_\gamma \cong E_o (1 + \tfrac{V}{c} \cos\theta) \tag{3.4}$$

As the angle is zero, cos θ becomes 1, and using v/c as calculated above, the boost in energy is small when compared to the 2^+ ^{24}Mg energy of 1.369MeV (ie an extra 72keV).

3.1.3 Target Production

The $p(^{23}Na, \gamma)^{24}Mg$ reaction requires a hydrogen target. There are several ways to make such a target, including a hydrogen gas target, a self-supporting polymer target $(CH_2)n$, ice, or metal hydride (eg titanium hydride). In order to manufacture a target with the relatively high areal density of hydrogen that is localized in space and can withstand currents of 30pnA or more as required, then only ice or TiH_2 are suitable for this experiment. Of these two, TiH_2 would be the best choice because ice can only withstand small currents and would need special equipment to mount in the target chamber (ie cold finger in vacuum). To manufacture the TiH_2 target, the following procedure [NIM 72] was carried out. Mount titanium foils totalling ~1g in a bell jar, then evacuate the jar. Heat the foils to 500°C to outgas material and then allow cooling to 400°C. Close off the high vacuum pump. Slowly introduce the hydrogen from a small lecture bottle into the bell jar and hold at 400°C for ten minutes. Slowly reduce the temperature over a period of several hours. The pressure of hydrogen is monitored to determine the uptake of hydrogen by the foils. After reaching room temperature, the system is slowly vented to atmosphere and opened. Any remaining hydrogen (<0.2l at STP) is dispersed into the room. Hydrogen will remain in the foil unless the foil is reheated.

3.1.4 Determination of gamma interaction position

The objective of the highly-segmented TIGRESS HPGe detector is to be able to correct for the Doppler shift of gamma rays emitted from recoiling nuclei produced in nuclear reactions initiated by accelerated radioactive beams. In order to achieve this, the location of the first interaction of an incoming gamma ray must be determined to within as small an uncertainty range as possible. The TIGRESS array will be capable of measuring these interaction points to better than a 2mm uncertainty for 99.2% of all single interactions. [Sve 04]

A catalogue of waveforms was produced in a separate experiment. The waveforms may be measured at localized interaction points in all three dimensions within the HPGe in order to determine the position sensitivity of the TIGRESS detectors. It is necessary to combine a collimated gamma-ray source in x and y with a coincident detector that determines the depth z in order to deduce the response of an HPGe detector to a particular deposition energy at a well defined three dimensional location. By positioning bismuth germanate (BGO) scintillators to view the HPGe clover through shielded slits, gamma rays scattering through 90° in the HPGe can be detected, and be determined to have well-defined depth values. Computer models show that the depth dependence of the pulse shapes vanishes in the coaxial region at the back of the detector so depth positioning has an effective cutoff at these depths. [Sve 04]

A well-defined energy is deposited at a well-defined three-dimensional location in the HPGe when combining a time coincidence between the HPGe and a BGO detector and having the proper energy division between two detectors, to provide a sample of events. One disadvantage of imposing this restriction is a low event rate. In order to generate a statistically significant sample of waveforms when testing a TIGRESS detector, approximately 2 months of data collection is necessary. [Sve 04]

The location of the gamma ray interaction was not necessary in this experiment because the detector was only used to record energies of the emitted gamma rays and not their positions. However, for the test on the TIGRESS detector, performed in July 2005, a $^{16}O(^{12}C,p\gamma)^{27}Al$ reaction was used. It was necessary to position the TIGRESS detector at 90^{o} to the beam and to have a silicon detector placed directly in front of the beam. The silicon detector recorded the energy of the protons, which travel in the forward direction. The TIGRESS detector recorded the energies of gamma rays. When a coincidence between proton detection and gamma detection was achieved, the waveforms for all the segments were recorded. When both events were present, energy from a ^{27}Al gamma ray was detected, signaling that this was a 'real' event.

Chapter 4

Experiment

4.1 Preliminary

In this chapter, a description of the experiment will be given and the methods described for the subsequent data analysis, along with the results obtained.

The beam was produced by the accelerator operators, who began by loading sodium into the ion source and heating it to produce a beam of 30pnA of 1.30 MeV/A. The intention was to start with the higher beam energy of 1.43 MeV/A, observe the resonance lines and then confirm that they disappeared at the lower beam energy. Since it was easier for the operators to begin with the lower energy and gradually increase it, it was decided to begin at 1.30 MeV/A. However, the appearance of the lines expected at the higher energy had already been established and the experimenters initially forgot that the beam was at the lower energy. Consequently, these lines would either not be present, or would be so weak as to be masked by the background; this is the case for the $2^+ \rightarrow 0^+$ transition in ^{24}Mg at a gamma energy of 1.37 MeV. Needless to say, none of the lines in ^{24}Mg and ^{20}Ne were detectable at this energy.

As has already been explained, the beam arrives in pulses or bunches separated by 90ns. An electronic signal was generated that measured the time between the detection of a gamma ray and the next beam pulse. This should be constant for all real events but random for background events. A time gate was set on the true time peak to reduce unwanted background events. The time spectrum was split to generate three gamma ray spectra - one spectrum gated directly on the time peak of the beam pulse (90ns central), one on the left 'wing' of the pulse (before) and one on the right 'wing' (after). Problems were encountered initially as separate components for data collection were not time-synchronized. Since the Ge crystals are very large, a significant number of the events result in very slow pulses. Rejecting these pulses improved the timing resolution. There were also some software difficulties, the analyzer and logger stopped working and the reset function would not respond, but these were all corrected early on.

After the beam energy was raised to 1.43MeV the expected gamma ray energy peaks were identified and a reassurance gained that the reactions that should have taken place were present. The lines expected to be seen initially, are represented in Table 4.1.

Gamma ray energy (MeV)	Isotope	Origin
0.44	^{23}Na	(p, p')
1.37	^{24}Mg	Resonance capture
1.63	^{20}Ne	(p, α)
2.75	^{24}Mg	Resonance capture

Table 4.1 Expected gamma rays

4.2 Procedure

The four targets prepared all had different properties. The first was titanium hydride (TiH) target, 11mg/cm^2 thick, the second was also TiH, 11mg/cm^2 but the target maker was not confident that the first target contained much, if any, hydrogen and could have been pure Ti, the third target was TiH but only 100 μg/cm^2. This one was thinner in order to populate only one resonance, with a dE of ~ 35 keV/A thick. The fourth target consisted of titanium only (ie no hydrogen). A Faraday cup was used to tune a 30pnA beam and then the target wheel was placed in the 8π target chamber and mounted on the end of the beam line. The target containing no hydrogen was aligned with the beam, set at 1pnA. A spectrum was taken. By far the strongest line observed was at 0.44MeV. This results from the Coulomb excitation of the ^{23}Na beam and confirmed that the beam was indeed sodium.

Having completed all the checks, the target was switched to one of TiH and a spectrum taken. The $2^+ \rightarrow 0^+$ and $4^+ \rightarrow 2^+$ transitions in ^{24}Mg would appear at 1.37 MeV and 2.75 MeV. If an alpha particle were emitted, one might observe the $2^+ \rightarrow 0^+$ transition in ^{20}Ne at 1.66 MeV. Also, if the pressure increased it would indicate loss of hydrogen from the target. (Obviously, this is undesirable but it would be evidence that the target DID contain hydrogen!)

The next target to be tested was TiH on Cu. There was no evidence that the target contained hydrogen. Lines from aluminium were in evidence so it was decided to try a Pb target to try and determine where the contamination from aluminium was coming from. Speculation was that it was coming from the end cap of the chamber or from the target housing. While the chamber was open, the opportunity was taken to try other targets. These were Mylar tape on Pb, thick plastic $(CH_2)_n$ on Pb and conducting Mylar tape on lead. It was discovered that the carbon in the plastic target produced a ^{33}S line from $^{23}Na(^{12}C, p, n)$, (evaporation fusion reaction), calculated to have a cross-section of 79mb. This should easily be evident when using a ^{23}Na beam and a C target. Some of the targets that were thought to contain no carbon were producing the sulphur line so the presence of carbon can probably be attributed to pump oil contamination, which contains hydrocarbons. When the beam was switched to the higher energy of 1.43MeV/A, the expected lines were indeed observed.

At the finish of this test, it was initially decided that a fusion evaporation reaction be used for the subsequent in-beam test with the TIGRESS prototype. The only drawback is that this reaction produces neutrons, which are damaging to a HPGe detector but this would not pose too great a problem because the yield of neutrons is sufficiently small and of low enough energy to not cause significant damage.

4.3 Data Analysis

On re-examining the data, it was found that when the beam was switched to 1.43 MeV/A the telltale lines indicating the presence of hydrogen were evident on the TiH Cu target. They were almost masked by the background however. The best run data were from Run 84, where data were collected for 165 minutes. The recorded data are held at TRIUMF so it was remotely accessed from McMaster University. Initially, Maestro software was to be used to aid in data analysis, as the author is familiar with this software. However, this caused a number of technical challenges and it was decided to use ROOT for the initial data analysis and to record each individual data point bin value, in order to reproduce spectra [Roo 04].

The line of greatest interest was the one at 2.75 MeV. This is the $p(^{23}Na, \gamma)\ ^{24}Mg$ resonance reaction and, as has already been discussed, is Doppler shifted by ~5%. Therefore, the line should be present at ~2.88 MeV. A spread in energy is expected, as the energy of each gamma ray is dependent on its angle with respect to the recoil direction. The line should not be present at a beam energy of 1.300 MeV/A, as this is below the threshold of the resonance, which occurs at an energy of 1.416 MeV.

Figure 4.1 shows a section of the spectrum collected during Run 84, where a number of peaks have been identified; they are also given in more detail in Table 4.2.

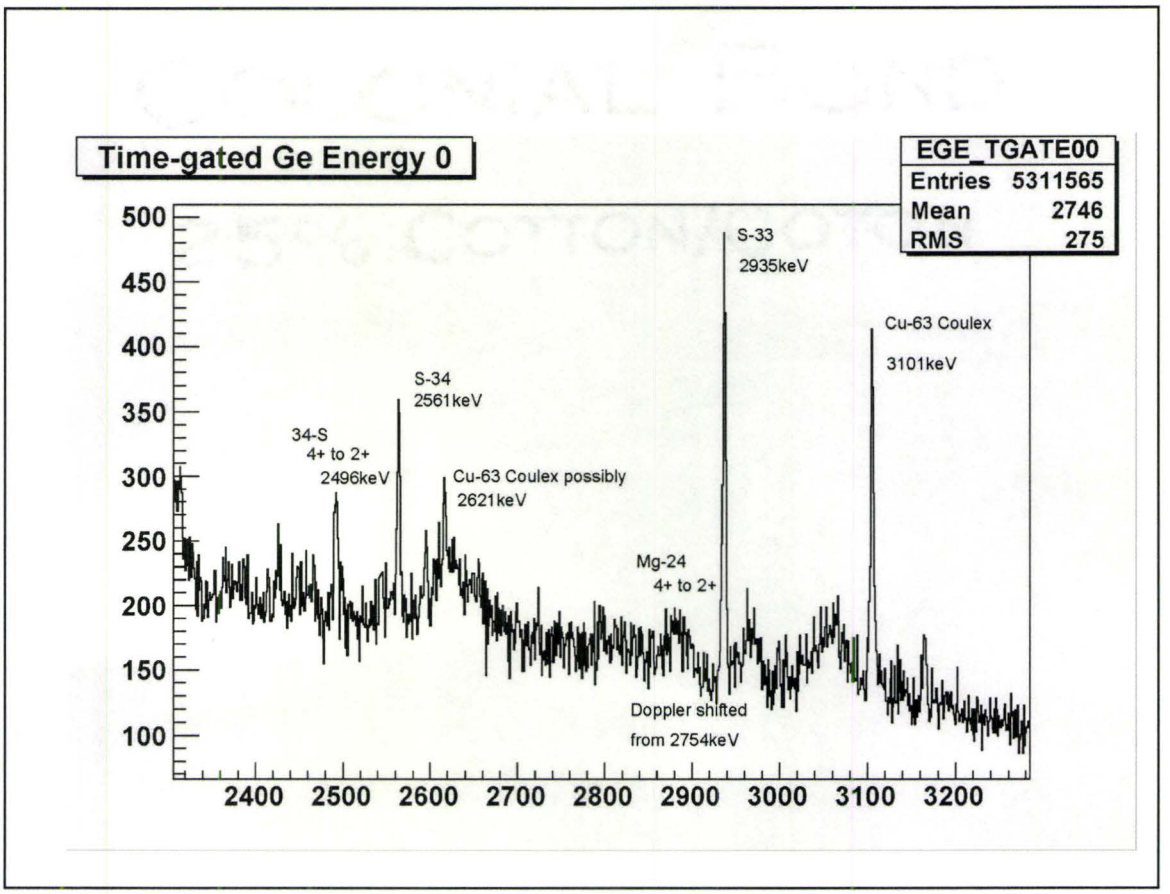

Figure 4.1 Spectrum showing identified peaks

Gamma energy (keV)	Isotope	Excitation	Reaction
2496	^{34}S	$4^+ \rightarrow 2^+$	$^{12}C(^{23}Na, p\gamma)^{34}S$
2561	^{34}S	$4^+ \rightarrow 2^+$	$^{12}C(^{23}Na, p\gamma)^{34}S$
2621	^{63}Cu	Coulex	
2754	^{24}Mg	$4^+ \rightarrow 2^+$ resonance	$p(^{23}Na, \gamma)\ ^{24}Mg$
2935	^{33}S	Fusion evaporation	$^{12}C\ (^{23}Na, pn\gamma)^{33}S$
3101	^{63}Cu	Coulex	

Table 4.2 Identified peaks

4.4 Results

4.4.1 Region of Interest

As previously mentioned, the Doppler shifted energy region around 2.88 MeV is of particular interest as this is the energy at which the resonance reaction is expected to be found. Microsoft Excel was adequate for the purpose of background subtraction. A comparison was made with an earlier run (Run 67), which was recorded at the lower beam energy of 1.30 MeV/A with the same target. There was no evidence at that energy of an energy peak at 2.88 MeV, as expected, and only one or two counts in equivalent bins; therefore these data are not included in the analysis. The background was subtracted using an adaptation of the "Total Peak Area with Extended Background Method". Subtraction of the background from the experimental data was performed because a background count with the target absent and the beam present is not a true representation of the background. This is because the majority of the background arises from Compton scattering of gamma rays produced by the beam interacting with the target, and is unique to each beam-target setup.

The total peak area chosen extended from 2.87 MeV to 2.90 MeV. The Doppler shift variation over this peak area was calculated, in order to verify that this was the correct peak. The variation in shift ranged from 3.5% at the lower energy to 5.9% at the upper energy, which of course includes the predicted Doppler shift of 5% of c.

The gradient of the background was calculated by using the equation of a straight line, giving a negative slope of -0.37+/-0.04. The uncertainty was calculated using standard error techniques. The net peak area was summed, giving a total peak count of C_{obs}=1024+/-150.

To find the quantity of hydrogen in the target, the stopping power is written as:

$$\Sigma = \Sigma_H + \Sigma_{Ti} \Rightarrow \Sigma = \Sigma_H + \frac{1}{x}\Sigma_{Ti} \cong \frac{1}{x}\Sigma_{Ti} \qquad (4.1)$$

where x is the ratio of hydrogen to titanium. The stopping power, Σ_H, of hydrogen makes a negligible contribution and can be discounted.

Using values derived in Chapter 2 section 2.2, Table 4.3 shows the derived and published values for calculating the yield.

E(MeV)	λ^2(cm^2)	$\omega\gamma$(eV)	Σ(Ti) (eVcm^2/atom)	resonances/ particle
1.416	6.30 x 10^{-24}	5.25	6.36 x 10^{-13}	2.60 x $10^{-11}x$

Table 4.3 Values used for calculating resonance yield.

The experiment ran for 165 minutes and so the total number of beam particles was, N=7.6x10^{14}. During this time, C_{obs}=1024+/-150 photons were detected in the

2.75MeV photopeak, as mentioned previously. The branching ratio for decay through this gamma ray is γ'=0.95 and the detector efficiency was estimated to be e=0.029+/-0.004. This results in a value for the resonances/particle of:

$$Y_{obs} = \frac{C_{obs}}{N\gamma e} = \frac{1024}{7.6x10^{14} \cdot 0.95 \cdot 0.028} = 4.9x10^{-11} \quad (4.2)$$

This number is to be compared to the value in Table 4.3, which gives a calculated number of resonances/particle and depends on the ratio of hydrogen to titanium in the target:

$$Y_{calc} = 2.60x10^{-11}\,x \quad (4.3)$$

The composition of the target can now be determined from the results of (4.2) and (4.3):

$$x = \frac{4.9x10^{-11}}{2.6x10^{-11}} = 1.9 \pm 0.5 \quad (4.4)$$

Since titanium metal is known to absorb hydrogen up to a ratio of 2:1 ie TiH_2, this value is reasonable.

Chapter 5

Conclusion and Future Prospects

Although the test was successful in detecting the $^{24}Mg\ 4^{+}\rightarrow 2^{+}$ resonance line at 2.754MeV, Doppler shifted to 2.880MeV, and in confirming the amount of hydrogen in the target, alternative approaches came to light during the analysis of this test, which will prove easier to prepare and carry out than using the initial combination of Na/C.

As has already been mentioned in Section 4.2, during one of the runs at the higher beam energy, it was noted that a peak at 2.94MeV was present, which would not normally be there from the hydrogen in the target. On closer inspection, it was discovered that this was a ^{33}S line from ^{23}Na on ^{12}C, ie $^{12}C(^{23}Na, pn\gamma)^{33}S$ (fusion evaporation reaction). It was concluded that the carbon came from the presence of pump oil in the vacuum chamber. The half-life of this gamma ray is 28fs, long enough to be stopped in the target, resulting in a sharp energy peak. When the configuration of ^{23}Na on ^{12}C was run through a computer simulation (PACE4), with a beam energy of 1.43 MeV/A, the ^{33}S line was found to have a yield of 57.7% and a cross-section of 88.5mb - much larger than anything else present, making it easy to identify. This indicated that fusion evaporation reactions would make a better choice for the actual in-beam test. Other combinations were simulated and the conclusion was that a ^{16}O beam on a ^{12}C

target be used where the $^{12}C(^{16}O, p\gamma)^{27}Al$ fusion-evaporation reaction will be initiated. This has a simulated cross section of 425mb with a yield of 77.4% at a beam energy of 1.7MeV/A. The disadvantage of using this reaction is that there are a lot of peaks at similar energies, which may not be simple to resolve.

5.1 Result expectations

Even though the test of the TIGRESS prototype detector has been carried out recently, in-depth data analysis has not yet been completed. Before the test was made, the author recommended the fusion evaporation reaction and made predictions of the outcome. From computer simulations, recommendations were made before the prototype test on various parameters, such as beam energy.

Different beam energies were simulated before it was concluded that 1.7MeV/A was the optimum energy for the desired reaction. It should be noted that the values calculated by PACE4 should only be used as guidelines and not compared directly with any experimental results. Some of the useful features in PACE4 are the partial cross section and angular distribution calculations for all residual nuclei identified. The way that the beam energy was chosen to be the optimum one was by looking at partial cross sections and determining which beam energy gave the largest spin cross section, ie how much angular momentum brought in what spin contribution and also from the total cross

section. Obviously, the upper constraint on beam energy is the maximum beam energy achievable at TRIUMF.

If a proton can be detected from the $^{12}C(^{16}O, p\gamma)^{27}Al$ reaction and its angle is known, then the angle of the recoiling nucleus will also be known. A silicon detector will be placed directly in front of the beam-target to detect protons. It is necessary to determine if there are sufficient protons being emitted within a solid forward angle corresponding to the face of the silicon detector so that there will be sufficient gamma rays detected by the TIGRESS detector in an associated angle range. This is because, once the proton has been detected, the associated gamma ray can be 'matched' to that proton and the recoil angle of the recoil nucleus is restricted. As the proton and the gamma ray are now associated the event will be verified as real. The recorded gamma energy can then be analysed and the Doppler shift subtracted. If the proton is emitted beyond the solid angle projected by the silicon detector, it will miss the detector and the associated gamma ray will be vetoed (not recorded as a real event).

Calculations were made to work out how many protons there were for a total of 100K cascades in 10° angle ranges from 0° to 30° at differing beam energies. It was decided that the calculations were only required out to 20° so the cross-section and scattering variation in angle of the nucleus at 20° was calculated. Table 6.1 shows the calculations made for beam energies ranging from 1.4 MeV/A to 1.9 MeV/A. Although

it is not yet possible to achieve the high beam energy at TRIUMF, the calculations were included to illustrate any trend.

E(MeV/A)	J_{max}	Counts at 10°	Counts at 20°	Total x-section	x-section at 20°	Scatter up to 3.5°
1.4	4	1728	4893	251	21.26	4899
1.5	5	1732	5117	318	28.09	5412
1.6	6	1826	5005	374	32.97	5639
1.7	6	1764	5219	425	38.26	7059
1.8	7	1850	5228	454	41.63	6834
1.9	8	1927	5569	477	45.93	6725

Table 5.1 Simulation calculations for ^{27}Al reactions

The scatter figures indicate how many of the ^{27}Al nuclei would have a variation in their angle from 0° to 3.5° from the 'kick' of the protons. The average angle was calculated using the following formula and was found to be 1.28°:

$$\Sigma \frac{c\theta}{c_{tot}} = \bar{\theta} \tag{5.1}$$

where c is the number of counts. This mean scattering angle for the proton gives the mean scattering angle for the ^{27}Al and needs to be small in order that the angle of emission is well defined.

By using the geometry of the beam to TIGRESS detector to calculate the variation in angle across the face of the detector, the variation in energy can be calculated. Each

crystal segment is 8cm in diameter and the detector is positioned 11cm from the target. This setup is illustrated in Figure 5.1:

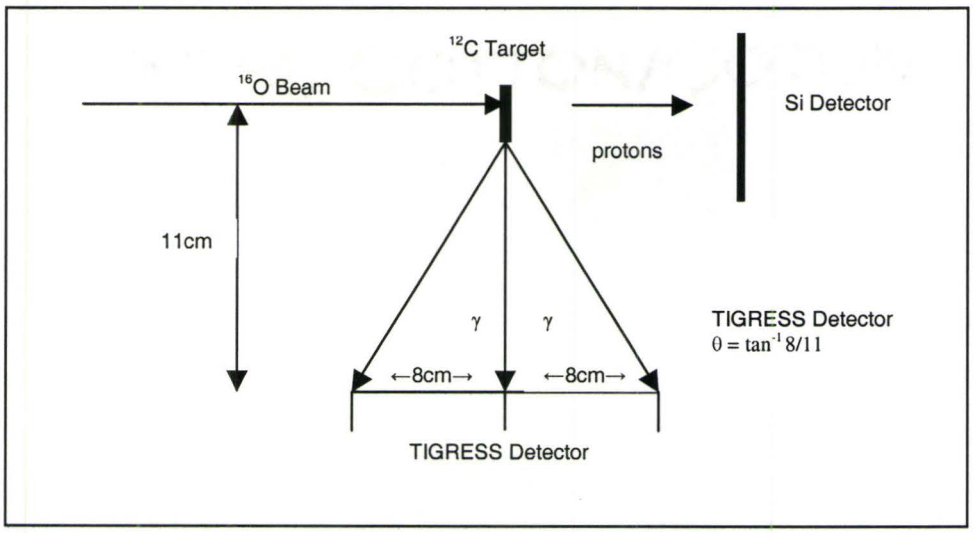

Figure 5.1 Geometry of summer test

The variation in angle is:

$$\pm \tan^{-1} \frac{8}{11} = 36^0 \tag{5.2}$$

Table 5.2 gives some examples of energies for differing Doppler shifts, scattering angles and depths into the detector for two examples of energies expected from the reaction, using equation (2.1):

E_o (MeV)	v/c (%)	Scatter angle (^{o})	$E\gamma_1$ (MeV)	$E\gamma_2$ (MeV)
0.980	2.5	0	1.000	0.960
0.980	2.5	-1.29	1.000	0.960
0.980	2.5	+1.29	0.999	0.961
3.000	2.5	0	3.061	2.939
3.000	2.5	-1.29	3.062	2.938
3.000	2.5	+1.29	3.060	2.940

Table 5.2 Examples of variation in energy

where $E\gamma_1$ is the maximum energy and $E\gamma_2$ the minimum. Calculations were also performed for variation in energy to a depth of 3mm into the detector but these were so similar to the above that it was unnecessary to include them here. It can be seen from the table that for an energy of 3.00 MeV, there will be a maximum variation in energy of 248 keV across the face of the detector (124 x 2 for two segments), giving a variation, or resolution of 1.55 keV/mm. This figure is not quite linear, but a good approximation. This indicates that there is a high enough variation per mm to be able to determine the position of the interacting gamma ray on the detector and produce a narrow peak from pulse shape analysis.

By using a ^{16}O beam on a ^{12}C target, some of the nuclei that are formed give off unwanted neutrons, which damage the detector. PACE4 was used to estimate the neutron flux that the detector would receive from this type of reaction. It was found to be ~4000 neutrons/100k cascades, over all space, which becomes ~450 neutrons/detector. This amount of neutrons will not cause any significant damage to the detectors.

Figure 5.2 shows a spectrum taken during the course of the TIGRESS experiment. The blue curves show unresolved peaks, as would be the case with a single un-segmented detector. The red curves show partly resolved peaks by making use of which crystals are hit in an event, and the black curves show better resolution by utilizing the segments within the crystal (crudely correcting for Doppler broadening). This figure clearly shows how two peaks, which are only separated by 22keV, can be resolved with this type of detector, even before sub-segmenting analysis has been performed. The full-width-half-maximum (FWHM) for each of the three peaks also demonstrates the refinement in resolution that can be achieved by the TIGRESS detector. In the 'un-segmented' peak, the FWHM is 15.3 keV, the 'partly resolved' peak gives a FWHM of 6.8 keV, and the 'crystal segmented' peak gives a FWHM of 5.3 keV giving an overall improvement of 300% in the resolving power [Ama 05].

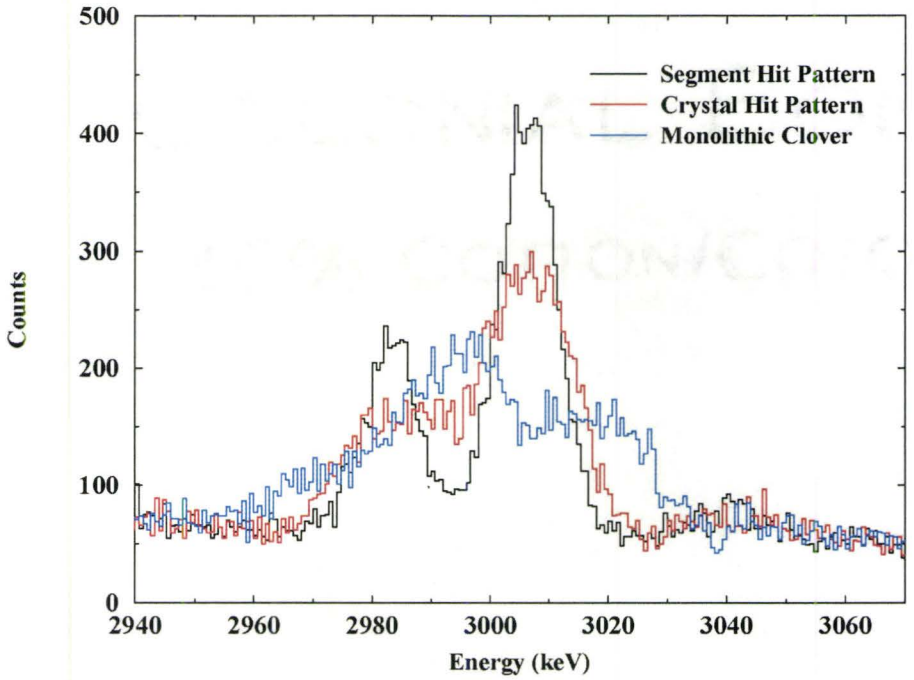

Figure 5.2 Doppler reconstruction of ^{27}Al peaks at ~3MeV. Adapted from [Sve 05]

The analysis of the TIGRESS experiment is beyond the scope of this work. However, from the preliminary analysis such as that shown in Figure 5.2, early indications are that the recommendations from this work proved beneficial to a successful TIGRESS detector test.

The purpose of this test was to find a suitable nuclear reaction to demonstrate the capabilities of the TIGRESS detectors. The process of selecting a suitable beam and

target has been described, and the results presented. Although the final recommendation was to use a different reaction in the subsequent in-beam test, this pre-test proved to be a valuable exercise in determining the ultimate choice of reaction, and also in predicting some of the expected results.

Bibliography

[Ama 05] P. Amaudruz, C. Andreoui, A. Andreyev, R.A.E. Austin, G.C. Ball, D. Bandyopadhyay, B. Barrett, C. Barton, J.A. Becker, L. Beaulieu, A.J Boston, P. Bricault, A.A. Chen, J. Chen, a. Chaffey, R.S. Chakrawarthy, R. Churchman, D. Cline, J.M. D'Auria, B. Davids, T.E. Drake, L. Erikson, P. Finlay, B. Fulton, P.E. Garrett, G.F. Grinyer, G. Hackman, B. Hyland, E. Illes, R. Kanungo, W.D. Kulp, A. Laird, C. Leroy, R. Maharaj, J.-P. Martin, C. Mattoon, E. McCullough, C. mercier, D. Morris, A.C. Morton, A. Noor, A. Olivieri, E. Paul, C.J. Pearson, A.A. Phillips, R. Prest, J.J. Ressler, R. Roy, F. Sarazin, H. Savajols, M.A. Schumaker, H.C. Scraggs, S. Seif El Nasr, M.B Smith, N. Starinsky, M. Strange, C.E. Svensson, J.J. Valiente-Dobón, J.C. Waddington, R.W. Wadsworth, L.M. Watters, S. Williams, J. Wong, and C.Y. Wu, TIGRESS Technical Progress Report, August 2005 (pre-publication). [Bri 01] P. Bricault, and M. Dombsky, CP600, *Cyclotrons and Their Applications 2001, Sixteenth International Conference*, American Institute of Physics 0-73543-0044-X/01, pp. 241-243, (2001).

[Bro 79] E. Browne, R. B. Firestone, Table of Isotopes, pub. John Wiley & Sons Inc, (1979).

[CEA 95] Evans Analytical Group website, hhtp://www.cea.com/cai/siminst/sources.htm *Copyright © 1995-2005 Charles Evans & Associates.*

[Dom 98] M. Dombsky, R. Baartman, P. Bricault, J. Doornbos, K. Jayamanna, T. Kuo, G. Mackenzie, M. McDonald, P. Schmor, and D. Yuan, Review of Scientific Instruments, V69, N2, pp. 1170-1172 (1998).

[Gre 99] P. Greenlees, Ph.D Thesis, University of Liverpool, (1999).

[Kee 99] A. Keenan, Ph.D Thesis, University of Liverpool, (1999).

[Les 04] H. Leslie, Resonance Reactions, Private Communication, (2004).

[Mey 72] M.A. Meyer, J.P.L. Reinecke, and D. Reitmann, Nucl Phys. **A185**, 625-643 (1972).

[NIM 71] P. M. Endt & C. van der Leun, Nuclear Instruments and Methods 97 (1971) 475-482.

[NIM 72] J.L. Gallant, Nuclear Instruments and Methods 102 (1972) 477-483.

[Nuc 70] K. Way (Editor) Nuclear Data Tables Volume 7, Number 3-4, (January 1970) 276.

[Roo 04] ROOT Version 4.02/02 – an object-oriented Data Analysis Framework, distributed under the liberal Open Source licence (LGPL LICENCE), Copyright © 1995-2004 Rene Brun & Fons Rademakers.

[Scr 04] H.C. Scraggs, C.J. Pearson, G. Hackman, M.B.Smith, R.A.E. Austin, G.C. Ball, A.J. Boston, P. Bricault, R.S. Chakrawarthy, R. Churchman, N.Cowan, G. Cronkite, E.S. Cunningham, T.E. Drake, P. Finlay, P.E. Garrett, G.F. Grinyer, B. Hyland, B. Jones, J. R. Leslie, J.P. Martin, D. Morris, A.C. Morton, A.A. Phillips, F. Sarazin, M.A. Schumaker, C.E. Svensson, J.J. Valiente-Dobón, J. C. Waddington, L.M. Watters, and L. Zimmerman, Nucl. Instr, Meth. A, p. 6, (2004).

[Sve 04] C.E. Svensson, G. Hackman, C.J. Pearson, M.A. Schumaker, H.C. Scraggs, M.B.Smith, C. Andreoui, A. Andreyev, R.A.E. Austin, G.C. Ball, A.J. Boston, R.S. Chakrawarthy, R. Churchman, N.Cowan, T.E. Drake, P. Finlay, P.E. Garrett, G.F. Grinyer, B. Hyland, B. Jones, J.P. Martin, A.C. Morton, A.A. Phillips, R. Roy, F. Sarazin, N. Starinsky, J.J. Valiente-Dobón, J.C. Waddington, and L.M. Watters, Nucl. Instr, Meth. A, pp. 3-5, (2004).

[Tig 04] Report on the TIGRESS Project Technical Review, private communication, (2004).

[Tri 02] Article: "TRIUMF expands research capacity", Paul Schmor, ISAC Division Head, The TRIUMF Newsletter, Issue Number One, Volume One, Fall 2002.

[Tri 02a] Index of /isac from web page http://www.triumf.ca/isac/isweb1-t.jpg.

[Tri 03a] Index of /isac from web page http://www.triumf.ca/isac/isac2-bldg-10mar03b

[Tri 03b] Index of /isac from web page http://www.triumf.ca/isac/isacIIa-02-medium.